Received: 27 August 2021 | Accepted: 30 August 2021

DOI: 10.1002/cnm.3529

SPECIAL ISSUE ARTICLE

WILEY

Patient-specific computational modeling of endovascular aneurysm repair: State of the art and future directions

Stéphane Avril[1] | **Michael W. Gee**[2] | **André Hemmler**[2] | **Sandra Rugonyi**[3]

[1]Mines Saint-Étienne, Univ Lyon, Univ Jean Monnet, INSERM, Saint-Étienne, France

[2]Mechanics & High Performance Computing Group, Department of Mechanical Engineering, Technical University of Munich, Garching, Germany

[3]Biomedical Engineering Department, Oregon Health & Science University, Portland, Oregon, USA

Correspondence
Michael W. Gee, Mechanics & High Performance Computing Group, Department of Mechanical Engineering, Technical University of Munich, Parkring 35, Garching 85748, Germany.
Email: gee@tum.de

Funding information
Bayerische Akademie der Wissenschaften, Grant/Award Number: pr48ta; Deutsche Forschungsgemeinschaft, Grant/Award Number: GE 2254/4-1

Abstract

Endovascular aortic repair (EVAR) has become the preferred intervention option for aortic aneurysms and dissections. This is because EVAR is much less invasive than the alternative open surgery repair. While in-hospital mortality rates are smaller for EVAR than open repair (1%–2% vs. 3%–5%), the early benefits of EVAR are lost after 3 years due to larger rates of complications in the EVAR group. Clinicians follow instructions for use (IFU) when possible, but are left with personal experience on how to best proceed and what choices to make with respect to stent-graft (SG) model choice, sizing, procedural options, and their implications on long-term outcomes. Computational modeling of SG deployment in EVAR and tissue remodeling after intervention offers an alternative way of testing SG designs in silico, in a personalized way before intervention, to ultimately select the strategies leading to better outcomes. Further, computational modeling can be used in the optimal design of SGs in cases of complex geometries. In this review, we address some of the difficulties and successes associated with computational modeling of EVAR procedures. There is still work to be done in all areas of EVAR in silico modeling, including model validation, before models can be applied in the clinic, but much progress has already been made. Critical to clinical implementation are current efforts focusing on developing fast algorithms that can achieve (near) real-time solutions, as well as ways of dealing with inherent uncertainties related to patient aortic wall degradation on an individualized basis. We are optimistic that EVAR modeling in the clinic will soon become a reality to help clinicians optimize EVAR interventions and ultimately reduce EVAR-associated complications.

KEYWORDS

aortic endovascular repair, computational mechanics, repair prediction, repair risk assessment, stent-graft simulations

1 | INTRODUCTION

When interventionalists and vascular surgeons decide on aortic repair, there is often (but not always) a choice between surgical open repair (OR) and a less invasive endovascular aortic repair (EVAR). In EVAR, a catheter with a crimped

stent graft (SG) is inserted in the circulation and directed to position using guide wires and in vivo radiographic imaging. Once correctly positioned, the SG is deployed into the desired portion of the aorta. SG deployment modulates blood flow and pressure away from the diseased aortic wall. EVAR today is the preferred method of repair and is commonly used in all sections of the aorta, for example, in treatment of thoracic and abdominal aortic aneurysms (TAA and AAA), aortic dissections (AD), as well as aortic valve replacements among other uses. EVAR was first described in 1991,[1] and has since been widely adopted in clinical practice due to being less invasive and exhibiting reduced in-hospital postoperative morbidity and mortality compared to OR.[2–9,30,31,44,45,51,52] However, EVAR requires long-term surveillance due to increased rates of late complications in comparison to OR. Complications of EVAR include late appearance of endoleaks,[8,16] SG migration,[17–19,21,27–29] as well as secondary formation of aortic dilatations at landing zones,[10,11,15,20] graft kinking resulting in occlusion of blood flow,[13,22] and SG fracture or disintegration of SG components,[19,23] all of which might require reintervention.[11–15] The mechanical behavior of the SG, pathophysiology of the aorta at the site of repair (such as abnormal geometrical, mechanical, and biological properties), and most importantly their interaction, play an essential role in the occurrence and individual likelihood of EVAR complications. There is an inherent large inner- and intra-individual variability, and thus uncertainty in the pathophysiological properties of the diseased aorta, because many if not most of the relevant parameters (geometric, mechanical, biological) can only be estimated to some extent in a patient-specific sense. These uncertainties pose both a challenge and an opportunity for predictive physics-based computational models of EVAR.

Challenges faced by computational modeling of EVAR include uncertainties in tissue properties; the highly nonlinear nature of the aortic wall behavior and its interaction with the SG, which also has complex mechanical properties; and tissue remodeling that occurs after EVAR placement. These uncertainties and challenges are also problematic for clinicians who estimate, based on previous experience and usual practices, the best SG size and positioning. Experience is key, and centers with a high volume of interventions indeed report reduced complication rates.[133,134] Nevertheless, complications after EVAR remain high.

Predictive computational models of EVAR thus promise to reduce uncertainties, and can aid in clinical decision making, providing an invaluable tool for clinicians. Furthermore, computational modeling can be used to tailor intervention strategies, including personalized SG designs, to individual patients, significantly reducing complications. While computational models of EVAR still need to evolve to achieve this promise, great progress has been achieved to date (some current examples include[171–174]). This manuscript will describe some current efforts at modeling EVAR using physics-based computational approaches and how these models are used to plan for EVAR interventions and predicting outcomes.

2 | ANEURYSM RUPTURE AND COMPLICATIONS AFTER INTERVENTIONS

The aorta is the main arterial vessel that connects to the heart and supplies oxygenated blood to the body. Because of the importance of the aorta in carrying blood, potentially life-threatening conditions occur when aortic tissues weaken leading to aneurysms, which are pathological dilations of the aortic vessel; or dissections, which are tears of the aortic tissue. Aneurysms and dissections can occur anywhere in the aorta (and other arteries), but are most common in the thoracic and abdominal aorta. Aneurysms and dissections need to be repaired to avoid aortic rupture, an almost always fatal event. Aortic rupture occurs when aortic wall stress exceeds aortic wall strength,[61–65,68,71,72,98] which is the stress at which the wall cannot longer withstand the forces applied to it, for instance forces from blood pressure acting on the luminal surface of the aortic wall. Rupture represents the main concern associated with TAA and AAA, as well as AD because rupture carries high rates of mortality (80%–90%), considering that most patients do not even make it to an aortic center on time.[99–104] Thus the goal of treatment is to repair the aorta before rupture occurs.

Criteria for elective AAA and TAA repair try to weigh the risk of aortic rupture versus the risk of repair. Repair has an in-hospital mortality rate of approximately 3%–5% for OR and 1%–2% for endovascular repair (EVAR) as reported in Greenhalgh et al.[9,116] in 2010 and 2001, respectively. Thus, the less invasive EVAR has become the preferred repair procedure. Four recent clinical trials in Europe and the United States [EVAR-1, DREAM, OVER, ACE], in which patients undergoing AAA elective repair were randomized for OR or EVAR, have indeed shown the early survival advantage of EVAR.[117] However, this early advantage was lost after 3 years post-intervention, mainly due to complications such as secondary rupture and reintervention in the EVAR group.[117,118] After 12 years of follow-up, survival rates dropped to about 40% for both groups, with rates of reintervention that continued to be higher for EVAR.[119] While early (30 day)

in-hospital mortality rates are about 3.4% for elective repair (OR and EVAR combined) and 33% for repair after rupture, there is no survival benefit or increased mortality of emergency versus elective repair after 30 days.[120]

Rate of complications after EVAR ranges between 16% and 30%, with secondary interventions needed in up to 19% of patients.[121] Because of these high rates of complications, patients undergoing EVAR require lifetime surveillance imaging, usually through computer tomography (CT) and ultrasound scans at 6–12 month intervals, in order to monitor for sac enlargement, graft displacement, and secondary rupture risk.[122] In addition to the inconvenience and radiation exposure associated with post-EVAR surveillance, long-term surveillance after EVAR is not practically feasible as 50% of patients become lost to follow-up after 5 years, and 10% never return after their EVAR procedure.[122]

One of the most common complications after EVAR are endoleaks.[121] Endoleaks occur when, after repair, blood continues to fill the space between the AAA or TAA sac tissue and the SG, leading to persistent pressurization of the aneurysmal sac and thus possible continuous sac growth and secondary rupture.[123,124] Endoleaks result from biomechanical factors, namely lack of proper sealing to prevent leakage of blood, and affect up to 30% EVAR patients.[121] Other frequent long-term complications are SG migration[17–19,21,131,132] as well as secondary dilatations of the aorta at the landing zones commonly leading to endoleaks,[10,11,15,20] graft kinking resulting in occlusion of blood flow[13,22] and SG fracture or disintegration of SG components,[19,23] all of which might require reintervention.[11–15]

3 | MODELING EVAR

Unsurprisingly, computational modeling of aortic treatment using EVAR has seen great and still increasing attention over the years. An overview of literature can also be found in.[25,26,37,38,41,42] This review intends to present an up-to-date overview of current methods employed in simulating different aspects of EVAR and provide a glimpse at future uses and development. Using computational techniques, specific challenging questions are addressed by means of predicting in vivo phenomena through a computational model, where the choice of model assumptions is governed by the question at hand and the availability of data and clinical trials for validation. Many model components are needed to perform in silico experiments on EVAR, which are briefly discussed in the following.

3.1 | Aortic wall models

The aortic tissue is composed of three layers (intima, media, and adventitia) with varying characteristics. In general, the orientation and crosslinking of collagen fibers and elastin content in the aortic tissue, mainly determine its mechanical behavior. An aneurysm, however, results from aortic wall tissue degradation and inflammation, that alter the mechanical properties of the aortic wall in ways that vary locally in the same patient, and are different from patient to patient. These mechanical properties depend on the degree of tissue degradation, which is unknown in an individual patient.[61,71,73,108,125] Moreover, the aortic wall may have calcifications that further alter its mechanical properties locally and globally. Additionally, the dilation of the aorta walls in aneurysms changes the characteristic blood flow in the aorta, and flow near the dilation becomes prone to thrombosis, generating an intraluminal thrombus (ILT) that lines the weakened aortic walls in most patients (80% of patients), shielding oxygen supply from the aortic wall and thus contributing to further wall degradation and increased risk of rupture.[135] When modeling aortic walls, therefore, all these factors (tissue degradation, calcifications, ILT) need to be accounted for in addition to the aneurysmal geometry.

Geometry of the vasculature is routinely captured in medical imaging using (phase contrast) CT, MRI, and ultrasound methodologies. There are various open source and commercial software solutions for segmentation of 3D models from CT or MRI image data sets, for example, MITK,[79] ITK,[80] Crimson,[82] Materialise Mimics,[83] Synopsys ScanIP,[84] and others, where usually some amount of user interaction is required to perform model segmentation. Output of segmentation is a surface description of the object of interest, for example, in the form of an STL surface tessellation that then can be further processed to create discretizations of the vascular model, see for example Figure 1.

From a modeling point of view, the aortic wall can be treated as an anisotropic fibrous composite, which consists of collagen fibers embedded into a ground matrix. The isotropic ground matrix accounts for all non-collagenous tissue contributors that impact the mechanical behavior of the tissue, such as elastin and smooth muscle cells.[109] Both two-fiber models (e.g., Haskett et al.[107]) and four-fiber models (e.g., Roccabianca et al.[108]) have been applied extensively for aortic wall models, where two or four families of collagen fibers are symmetrically aligned in the axial direction without contributors in the radial direction. In the last two decades, collagen fiber dispersion has been included into the models

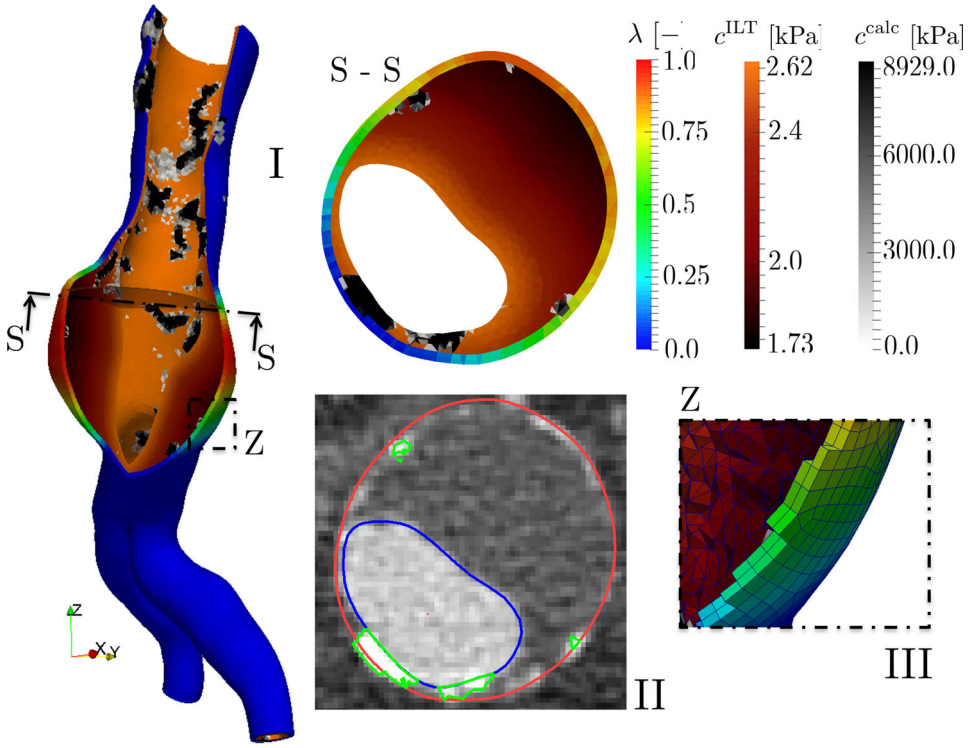

FIGURE 1 Exemplary model of a patient-specific abdominal aortic aneurysm. (I) Cut view of the vessel model and visualization of the different vessel constituents with color code: "healthy" aortic vessel wall (blue), aneurysmatic vessel wall (red), intraluminal thrombus (ILT) (brownish), and calcifications (gray scale). Here, a blending function λ was used to blend from a "healthy" to aneurysmatic material model based on distance to the luminal centerline. (II) Transversal CT image and model segmentation. (III) Detail view of a finite-element mesh. Figure reproduced with permission from Hemmler et al[48]

as a key contributor to the mechanical response of the aortic wall.[75–78] AAA progression is usually associated with a loss of elastin[72,125] as well as structural changes of the elastin and collagen fiber network[72,156] with increased fiber dispersion[17,57] leading to a more isotropic behavior. Thus simplified isotropic models are widely used for AAA wall modeling [63,72,136].

In the context of computational EVAR, both the properties of "healthy" and aneurysmatic aortic walls are of high importance. Holzapfel et al.[17,57,77] recently published an aortic wall model that can be fitted to data of "healthy" and aneurysmatic walls. A more practical approach to tackle the combination of "healthy" and aneurysmatic aortic wall properties was stated in Hemmler et al.,[47] where a general framework was provided to combine any "healthy" aortic wall model and any aneurysmatic wall model using a smooth-blending function based on the local radius of the aortic wall.

Many studies have been published on constitutive modeling of ILT in the past (e.g., Gasser et al.[110,111]), where the experimental and numerical study by Gasser et al.[110] with $n = 112$ specimens is probably the most elaborate. A detailed literature review on modeling of calcifications can be found in Maier,[112] where in general implicit and explicit modeling of calcifications is distinguished. Explicit calcification models (e.g., Deputter et al.[113,114]) treat calcifications as separate constituents with the drawback of challenging discretization of the mostly irregularly shaped calcification spots. In contrast, implicit calcification models,[112,115] do not use a separate constitutive model for calcifications. Instead, the stiffness of calcifications is considered by locally adapting the constitutive law.

3.2 | Stent-graft models

Because of the characteristics of aneurysms, stent-grafts (SGs) used to repair them are composed of stent wires that allow the SG to properly attach to the aortic wall and stay open, and a flexible material that excludes blood flow from the aneurysmal region effectively sealing the aneurysm. The materials employed and the SG design have to be such that they allow the SG to be crimped within its delivery sheath during placement, and then properly expand during

deployment. Common materials of commercial SG devices are stainless steel or nitinol for the stent wires and woven polyethylene terephthalate (PET) or expanded polytetrafluoroethylene (ePTFE) for the graft.

Homogenous SG models (i.e., one single homogenized material used for both stent and graft without resolving the detailed geometry and properties of stent and graft) were applied in the first computational EVAR studies for the sake of simplicity. Despite their frequent use in studying the interaction between SG and blood flow applying computational fluid dynamics (CFD) or fluid structure interaction (FSI) techniques[28,31–33,55,56], these models fail in reproducing the realistic mechanical behavior of SGs since the metallic stent and the membranous fabric graft have very different mechanical behaviors.

Recently, more elaborated multi-material SG models were applied[23,25,39,47,59,87,92–95]. These models are indispensable if the realistic mechanical behavior of the SG, including buckling of the graft, is of relevance.

For simplicity, the anisotropic material behavior of woven PET grafts is frequently approximated by isotropic elastic models.[23,25,47] In contrast, a more elaborated in-plane orthotropic elastic model was proposed by Demanget et al.[92–95]

Auricchio et al.[96,97] developed a superelastic constitutive model of nitinol applicable to stent modeling,[23,25,58] that accounts for the phase transformation between the austenitic and the martensitic phase associated with this type of shape memory alloy. However, in complex applications of SG models (e.g., SG deployment in patient-specific aorta) nitinol is frequently modeled as an elastic material.[48,60] This simplification seems to be reasonable for pure SG deployment simulations, when the interest is in the interaction between the stent and the aortic wall, since the phase transformation into the martensitic phase only occurs in the crimped state of the SG within its delivery sheath or during temperature changes.[60]

In many commercial SG devices, the stress-free stent diameters are larger than the stress-free graft diameter on which the stent rings are attached. Consequently, residual strains and stresses exist within the stent and graft in the unloaded assembled SG, which need to be addressed to precisely model the mechanical behavior of the SG. This property is usually denoted as stent pre-deformation[47] or stent preload.[39] In recent years, different approaches to account for stent pre-deformation were used. Roy et al.[39] doubled the stent Young's modulus which is rather a rule of thumb than reflecting the real effect of stent pre-deformation. In Derycke et al.,[89,94,95] SG assembly simulations, which are able to correctly account for the stent pre-deformation, were implemented. However, additional computational effort was required for the SG assembly simulation. In contrast, in Hemmler et al.[47,48] the stress-free diameter of the stent is correctly considered by means of a parameter continuation approach to fully account for the stent pre-deformation effect without having to perform an additional SG assembly simulation.

3.3 | Models of EVAR placement

For a large variety of in silico EVAR studies, the results of the intra-interventional EVAR steps are not the focus of interest. Accordingly, several different models of the EVAR placement have been developed to predict the final post-interventional state of SG and aorta after EVAR, rather than precisely replicating all single steps of the real-world EVAR procedure. These models of EVAR placement have to tackle numerically challenging contact scenarios between the SG and aortic tissue, buckling of the thin graft, and other sources of nonlinearities. To solve these numerical challenges within an acceptable time effort, different EVAR placement models have been developed. Early works by Figueroa et al.[27–29] artificially inflated the vascular geometry by a virtual pressure until the undeformed SG geometry entirely fits inside the vascular geometry without touching it. Then, this "helper pressure" is removed and SG makes contact with the arterial wall under physiological conditions, simulating the deformations and stresses in the wall and SG. All other EVAR placement models use computationally efficient morphing algorithms. Depending on the way in which the SG is placed in silico in the interior of the aorta (i.e., not following real-world procedure but rather algorithmically convenient ones), available models of EVAR placement can be subdivided into three different methods: *virtual catheter method*, *virtual shell method*, and *direct placement method*.

Early EVAR models adopted the so-called *virtual catheter method* from models of pure stent placement[85,86]. The *virtual catheter method* uses a cylindrical delivery catheter whose deformation during the SG placement process is fully prescribed. The virtual catheter is applied to radially crimp the SG, position the SG onto the aortic centerline, and finally deploy the SG in the interior of the aorta by enlarging the diameter of the virtual catheter again, see Figure 2.

Perrin et al.[88] developed a different model for EVAR placement and applied it to multiple real-world patient-specific cases.[58,60,89,90] In this so-called *virtual shell method*, first a discretized virtual tubular shell is placed around the SG. Using a suitable morphing algorithm, the virtual shell is morphed to the luminal vessel wall surface of the patient's

pre-interventional vessel geometry while contact constraints force the SG to stay inside the virtual shell during the virtual shell transformation. Finally, aortic wall material properties are applied allowing the aortic wall to deform elastically in response to the radial force exerted by the SG, see Figure 3.

Hemmler et al.[47,91] developed an EVAR placement model which fully avoids modeling of additional SG placement and crimping tools such as virtual catheters. Instead, in this so-called *direct placement method*, the SG is placed in the interior of the aorta by direct application of displacement constraints to the SG resulting from a 3D morphing algorithm, see Figure 4. After the SG deployment (removal of displacement constraints), both SG and aorta are treated as elastically deformable bodies subjected to stationary, physiologically meaningful, blood pressure states. The applicability of the *direct placement method* was demonstrated with patient-specific cases,[44,48] SG and AAA parameter studies[45] as well as SG customization.[46]

All three methods have been validated on small cohort basis[25,48,58] without showing significant differences in their predictive accuracy. While in general all three methods are able to predict the essential SG-related EVAR complications

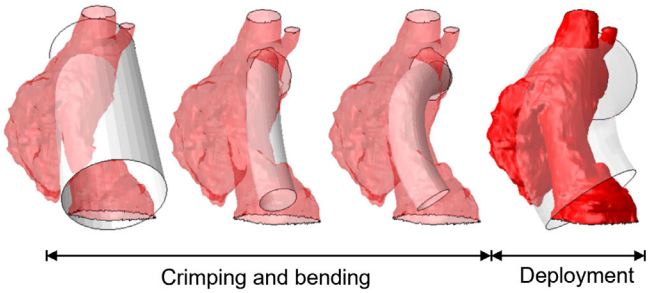

FIGURE 2 Simulation steps of the *virtual catheter method* applied to a patient-specific ascending aortic pseudoaneurysm. Color legend: virtual catheter (white), pseudoaneurysm (red). The SG is not visible in this figure. Figure reproduced with permission from Auricchio et al[25]

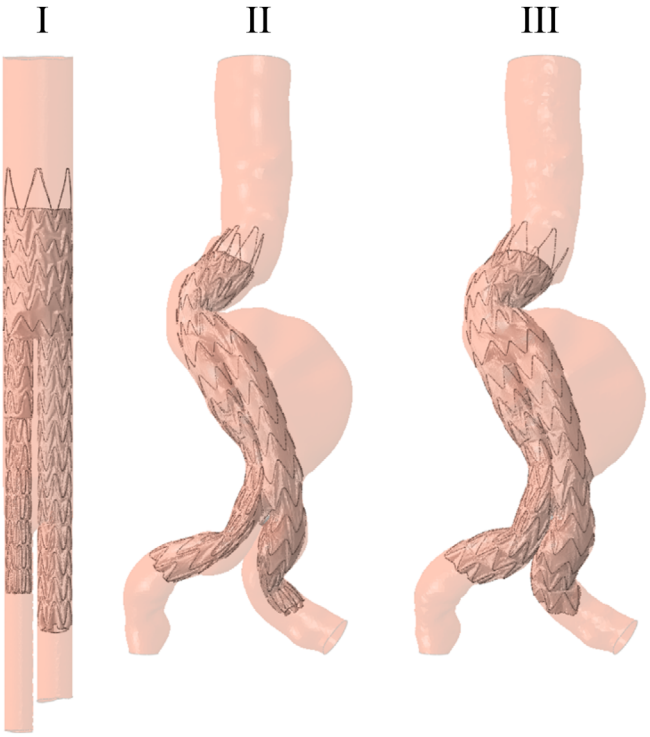

FIGURE 3 Simulation steps of the *virtual shell method* applied to patient-specific AAA: SG insertion and positioning in the tubular virtual shell (I), mesh morphing of the virtual shell from tubular shape to actual pre-interventional geometry (II), static mechanical equilibrium (III). Figure reproduced with permission from Perrin et al[58]

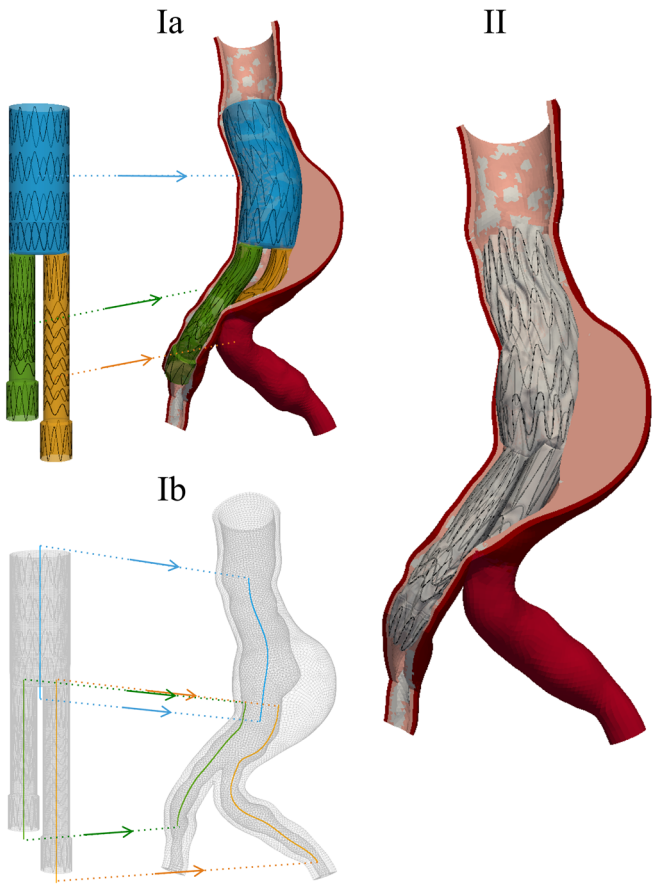

FIGURE 4 Simulation steps of the *direct placement method* applied to patient-specific AAA: placement of the SG (Ia) by direct application of displacement constraints to the SG using 3D morphing algorithm based on SG and AAA centerlines (Ib), static mechanical equilibrium. Figure reproduced with permission from Hemmler et al[48]

(e.g., SG malappositions, graft kinking, and SG-induced tissue overstress), the application of the virtual catheter method in the context of EVAR models[25,36,59,87] is mostly limited to non-bifurcated SGs since for bifurcated SGs several virtual catheters are required[43] and the complexity increases significantly. Further, in Perrin[88] it is shown that the virtual shell method is computationally more efficient than the virtual catheter method since it avoids modeling of the delivery catheter and its complex contact with the SG. The direct placement method further reduces the computational complexity since during the in silico SG placement, the deformation of the SG is fully prescribed by displacement constraints. This enables the use of implicit finite-element methods (FEM) while for the virtual catheter method and the virtual shell method mostly explicit FEM is used. Further advantages of the direct placement method are its combined use of computationally efficient stent pre-deformation and SG parameter continuation.[47] Last but not least, the choice of method also is governed through the choice of FEM software framework. A commercial FEM software would be less flexible and more restricted with respect to methodology than an open source software framework (or in-house), where every aspect of the code can be manipulated and augmented. It seems that the virtual catheter method is more suitable to be implemented in a commercial software framework, while virtual shell and direct placement method are more demanding with respect to software flexibility.

3.4 | Methodological challenges in computational EVAR

Computational EVAR is subject to several methodological challenges, which are briefly summarized in this section. First of all, SG placement and deployment is a highly nonlinear process, which requires advanced numerical methods as well as suitable and efficient solvers to satisfactorily simulate the large displacements and nonlinear behavior in a reasonable time frame. Nonlinearities mainly arise from the buckling of the membranous graft, the

complex contact scenarios between SG and the aorta wall, as well as the nonlinear material behaviors of the aorta and SG components. Apart from these computational challenges, in vivo stress-free aortic geometries[66,67,70,100] as well as residual stresses arising from the stent pre-deformation effect[39,47] need to be addressed by suitable computational methodologies. As mentioned before, patient-specific aortic properties, such as the aortic wall thickness and the aortic wall stiffness and collagen dispersion, are usually difficult to estimate and therefore mostly treated in terms of population-averaged quantities instead of patient-specific ones. Some studies address these aortic uncertainties with probabilistic approaches[49,61,71] in the context of patient-specific AAA rupture prediction. Incorporating these probabilistic approaches into computational EVAR, however, would drastically increase the computational effort. Finally, the high complexity of patient-specific aortic and SG shapes is additional challenges in computational EVAR. This geometrical complexity makes automatic model generation an ambitious task, but one that is essential for the application of EVAR model prediction in clinical practice. Many of the mentioned challenges are specific to EVAR simulations and hard to incorporate in existing commercial simulation software. Thus, most of the cited work by various groups have utilized their own software frameworks or have made complex and effortful modifications to open source software frameworks. This somewhat hinders commercialization and wide-spread application of such computational tools in clinical practice and multicentered studies, as well as larger-scale community efforts.

4 | PREDICTIVE MODELING IN CLINICAL APPLICATIONS: MITIGATING EVAR COMPLICATIONS AND OPTIMIZING EVAR PROCEDURES

Computational analyses of EVAR interventions (structural, fluid, or both) in AAA, TAA, or AD all aim at making predictions that can reduce the risks and likelihood of EVAR complications, see Figure 5. In the preoperative planning of EVAR interventions, practitioners must choose the appropriate SG type and sizes to ensure that the aneurysm is completely sealed without covering important collateral arteries, particularly renal arteries at the proximal landing zone and internal iliac arteries at the distal landing zone. Numerical analyses should be able to predict beneficial SG oversize and potential bending or kinking. It is also critical to anticipate complications that may arise over time. For that, numerical analyses should be able to predict post-EVAR hemodynamics in the aorta or in the relevant branches, aortic remodeling due to the interaction of SGs and artery walls, drag forces on the SG, and potential development of endoleaks.

Such predictions are still a work in progress, in the next subsections we review some current applications. These include applications in which numerical analyses have permitted us to optimize SG designs in order to improve or optimize EVAR outcomes.

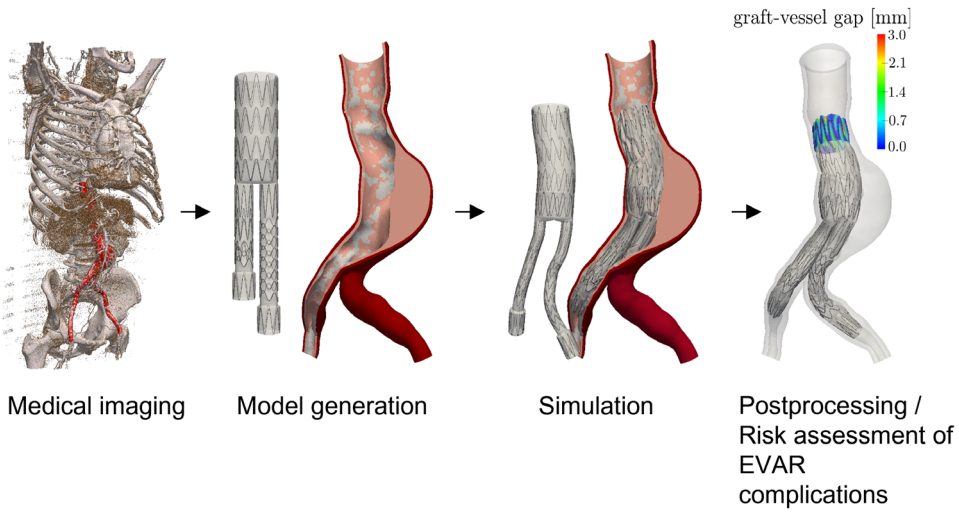

FIGURE 5 General process workflow of predictive EVAR modeling from model generation to the postprocessing of the simulation results. Figure reproduced with permission from Hemmler et al[44]

4.1 | Simulating the insertion of delivery systems, graft deployment, and prediction of defects in graft positioning

During EVAR procedures, the insertion of guidewires and delivery systems, and SG deployment are usually performed under 2-D fluoroscopic imaging, which enables visualization of bone structures and radiopaque tools. Recently, advanced imaging systems have been developed, which allow the fusion of CT angiogram images with live fluoroscopy that can then be used as an arterial roadmap to facilitate endovascular navigation.[137–140] However, stiff guidewires usually deform iliac arteries and even the aorta such that the preoperative CT scan does not reflect anymore the current arterial geometry.[141–143] It is critical to predict these deformations using computational analyses as otherwise, surgeons can only anticipate these deformations based on their experience.

A number of publications proposed biomechanical models and methods to predict the deformations caused by guidewire insertion during EVAR procedure.[40,53,105,106,130,144–148] Among them, Gindre et al.[105] were the first to present an evaluation of modeling results against quantitative patient-specific intraoperative data. Their numerical framework takes into account blood pressure pretension and external support modeling and can simulate real interventions.

Virtual SG deployment simulation, using pre-interventional CT angiogram and finite-element simulations of SG deployment, can mimic biomechanical interactions between SG and the aorta during an EVAR procedure and provide quantitative prediction of SG position and wall stress, see for example, Figure 6. This application, with the objective of assisting in EVAR procedures, is by far the one that received the largest number of publications.[47,48,58,60,87,93,149,150] Latest developments in SG deployment modeling are related to reducing the computational time required for simulations, as this is a major limitation for using these simulations in the operating room.[24,151]

4.2 | Simulations of AAA tissue deformation and remodeling after EVAR interventions

An extensive literature on growth and remodeling (G&R) of aortic tissue exists,[18,50,54,125–129,152–154] mostly independent of the EVAR question at hand. In 2005, Li and Kleinstreuer[33] were the first to achieve FSI analyses of AAA and SG following EVAR. They showed that AAA peak wall von Mises stresses were reduced by a factor of 20 once the artery was excluded from blood flow. Their models, based on idealized/smooth AAA geometry and SG with uniform isotropic properties, were accurate enough to demonstrate disturbed flow (with recirculations), identify pressure and velocity profiles, and drag force on SG. Their model did not account for a real patient-specific (tortuous) geometry, along with ILT and calcifications. More recently, Hemmler et al.[45,47,48] developed a suitable in silico EVAR methodology for patient-specific cases that can be used to predict SG-related complications, such as endoleaks or tissue remodeling-induced aortic neck dilatation. Their sophisticated models of patient-specific vessels included ILT, calcifications and an anisotropic model for the vessel wall. They validated their model against the position of stents imaged with post-interventional CT and were the first to evaluate SG-induced tissue overstresses in patient-specific aortas, see Figure 7.

Shrinkage of the aneurysm sac is commonly accepted as clinical evidence for a successful EVAR. However, there is also a pressing need to simulate aneurysm evolutions after SG implantation, especially considering the recent advances

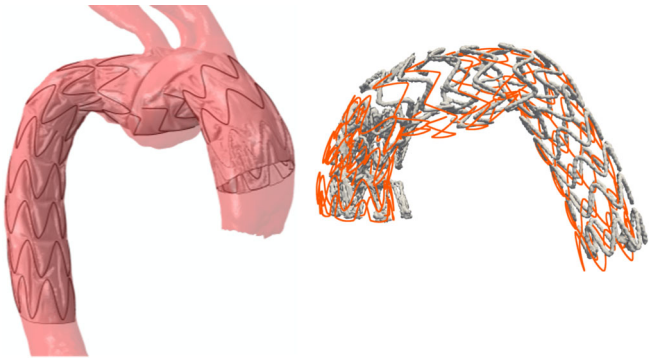

FIGURE 6 Result of the virtual deployment of a double branch SG in a patient-specific aortic arch aneurysm (left). Superimposition of the stent rings segmented from the post-interventional CT scan and from the simulations (right). Color legend: post-interventional CT (gray), simulation results (orange). Figure reproduced with permission from Derycke et al[89]

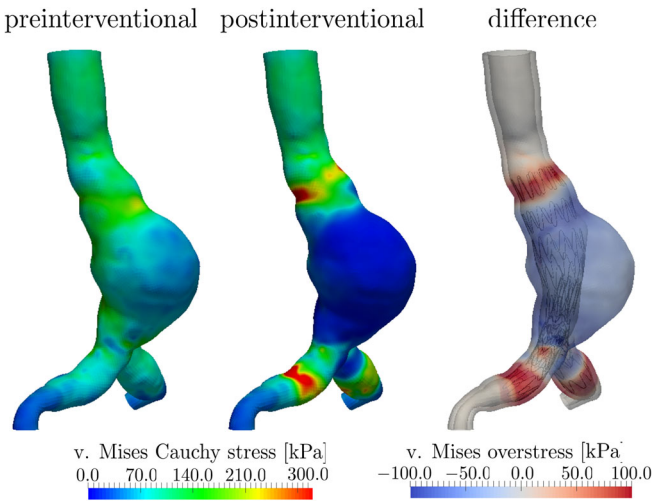

FIGURE 7 Aortic wall stress comparison of a patient-specific AAA treated by a bifurcated Cook Zenith SG at 130 mmHg blood pressure: aortic wall von Mises Cauchy stresses before EVAR (left), aortic wall von Mises Cauchy stresses after the virtual SG deployment (middle), SG-induced aortic wall von Mises overstress as difference between the post-interventional stress and the pre-interventional stress. Figure reproduced with permission from Hemmler et al[48]

in G&R computational models.[152–155] Numerical models can be an interesting alternative option for studying influencing factors in sac expansion/shrinkage. Only one numerical model has ever been published on aneurysm adaptation after EVAR.[156] In that original study, a 2D finite-element axisymmetric shell model was developed for simulating G&R after stent-graft implantation. The main drawback of this model was to be 2D, which prevented its application to patient-specific cases and validation.

4.3 | Simulations of post-EVAR blood flow dynamics

The earliest applications of computational studies on EVAR were CFD analyses related to the prediction of drag forces on SGs as well as possible endoleaks and their effects.[10,32–34,55,56,157–159] This is a logical first step as migration issues were critical for first generation SGs. While some of these issues have been solved by manufacturers, predicting the drag forces remains critical for the durability of Fenestrated-EVAR (F-EVAR). F-EVAR was introduced because some patients are not suitable for EVAR due to hostile AAA morphology. Kandail et al.[160–162] conducted a numerical study where they computed, using CFD, the displacement forces acting on fenestrated SGs, based on patient-specific geometries reconstructed from CT scans. Although displacement force arises from blood pressure and friction due to blood flow, numerical simulations can elucidate the net blood pressure, which is the dominant contributor to the overall displacement force. They showed that while loads exerted by the pulsatile flow dictates the cyclic variation of the displacement force, its magnitude depends not only on blood pressure but also the fenestrated SG morphology, with the latter determining the direction of the displacement force.

Hemodynamics in the aorta as well as in target vessels such as the renal arteries may also be a major concern in F-EVAR and chimney EVAR (Ch-EVAR), see for example, Figure 8. Renal events, such as target vessel loss (3–4%), renal stenosis (7%), or postoperative renal dysfunction (20%–29%) often complicate complex EVAR.[163–166] Renal dysfunction may arise from perioperative arterial lesions caused by the device or from strong hemodynamic alterations following the procedure. Intrastent stenosis and thrombosis after stent implantation remain major clinical issues. Wall motion and flow disturbances distal to the SG are associated with increased intimal hyperplasia, particularly at the junction between the stent and the artery. The mechanisms are not fully understood, but direct endothelial damage, reduced compliance, alteration of the distribution of the wall shear stress (WSS) within the SG[167] may be involved. The stent rigidity relative to the native arterial compliance results in stiffness mismatch,[167] which may stimulate intimal hyperplasia.[168]

Analyzing renal artery hemodynamics following F-EVAR may help to understand the occurrence of renal complications such as intrastent or arterial stenosis from intimal hyperplasia or thrombosis in the renal arteries. To assess the

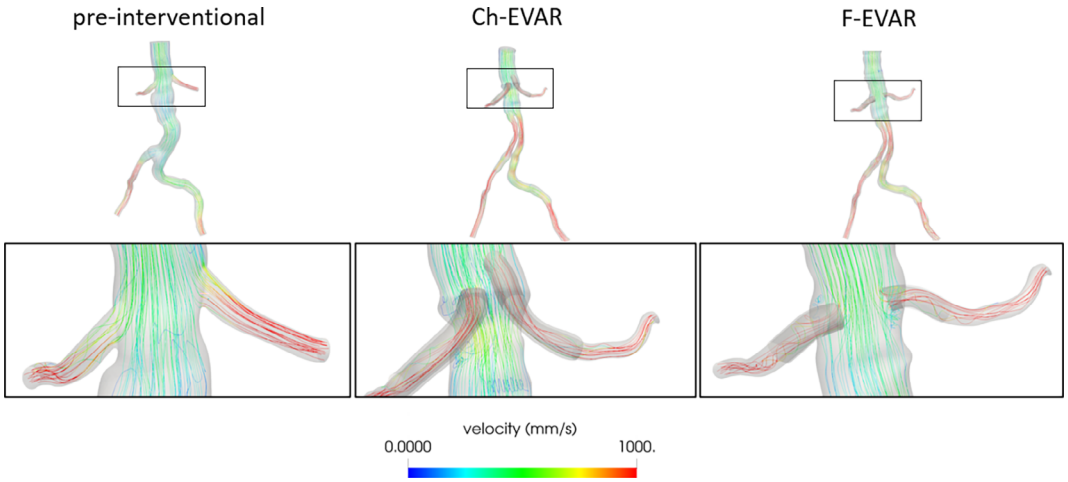

FIGURE 8 Comparison of the Ch-EVAR technique and the F-EVAR technique for a patient with complex AAA anatomy using CFD. Hemodynamics in the abdominal aorta and renal arteries before EVAR (left), after Ch-EVAR (middle) and after F-EVAR. Vessel and SG walls were modeled as rigid, blood was treated as a Newtonian and incompressible fluid. A pulsatile adapted patient-specific flow waveform was prescribed at the aortic inlet using a Womersley velocity profile. Outflow boundary conditions were prescribed using three-element-Windkessel models coupled to each outflow branch (renal and iliac arteries)[177]

hemodynamic outcomes of branched SGs (BSGs) for different anatomic variations, Kandail et al.[160–162] constructed idealized models of fenestrated stent-grafts (FSGs) with different visceral take-off angles (ToA) and lateral aortic neck angles. They concluded that the blood flow rate in renal arteries depends on the configuration of the SG, with a retrograde configuration resulting in slightly lower renal flows.

4.4 | EVAR SG customization aided by computational mechanics tool

In most high volume aortic centers, EVAR SG implantation is considered the first line treatment for TAA and AAA in patients with suitable anatomies. To treat complex AAA with unfavorable anatomies (short infrarenal neck, suprarenal, or type IV thoracoabdominal aneurysms), custom made devices specifically tailored to each patient's anatomy, such as F-EVAR, are needed (more than 20% of EVAR interventions). As a result, delay for planning and manufacturing currently ranges from 6 to 8 weeks, which may preclude its use in patients presenting with large aneurysms. Accurate device planning requires the use of dedicated three-dimensional imaging software combined with a high resolution preoperative CT scan to perform all the necessary measurements. In patients with arterial tortuosity or important angulation, it is difficult to predict SG behavior in the aorta.

Planning software allowing SG sizing based on geometrical measurements, lengths, and diameters exists in the SG manufacturing industry, but may not be sufficient to propose an appropriate customization of SGs in such situations as the mechanical outcome in the tissue and fluid mechanics is only anticipated qualitatively based on experience. Virtual SG simulation models are thus needed as an interventional planning tool.[169] Such simulation tools are based on finite-element analysis (FEA) to predict the deployment of SGs in aortic aneurysms.[47,48,58,60,87,93,149,150] The development of these FEA simulations to assist cardiovascular interventions started less than a decade ago. Mechanical properties were characterized using bench tests and used to achieve FEA analyses of SG deployment in virtual aortas and iliac arteries. Recent literature has highlighted the advances in customizing EVAR and suprarenal devices deployed in virtual models, even permitting now automated sizing of FSGs.[90]

Hemmler et al.[46] performed an in silico study comparing off-the-shelf SGs and customized SGs qualitatively and quantitatively in terms of mechanical and geometrical parameters such as stent stresses, contact tractions, and fixation forces. The numerical investigation has shown large benefits of the highly customized SGs compared to off-the-shelf SGs. In particular, they showed that customized SGs achieved better SG-vessel attachment and a considerable increase in SG fixation forces of up to 50% than off-the-shelf SGs, which indicate decreased likelihoods of EVAR-related complications, see Figure 9. Besides the frequently investigated optimal degree of SG oversizing (see, e.g., Prasad et al.[35,45,150]), this study highlights that the optimal SG design should have the same morphology as the local morphology of the vessel

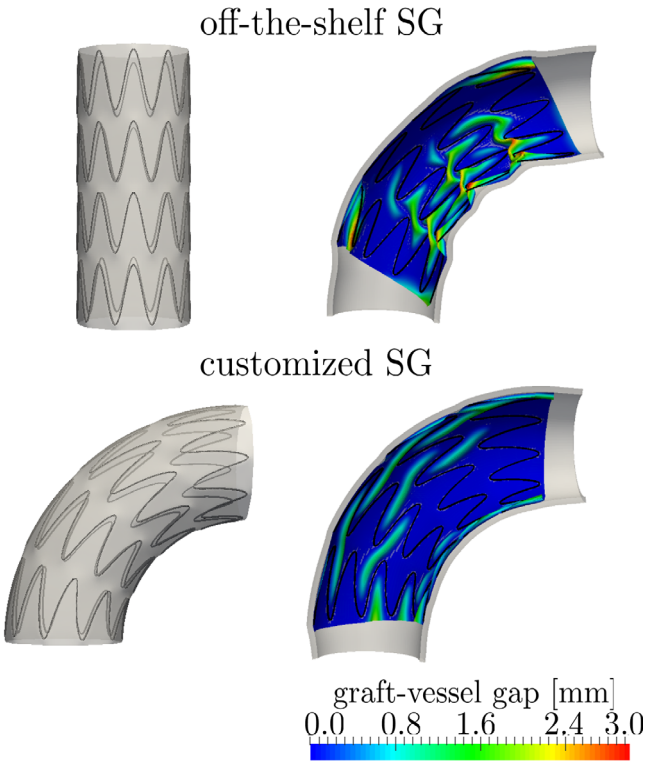

FIGURE 9 Virtual SG deployment of a straight off-the-shelf SG (top) and a highly customized curved SG (bottom) in a curved aortic segment. Comparison of the gap between aorta (gray) and SG (rainbow color scale) in the deployed state for the two SG cases. Figure reproduced with permission from Hemmler et al[46]

in the landing zone where the SG is placed. For instance, in case of a conical vessel-landing zone, a conical SG is preferable to a standard cylindrical one.

In thoracic EVAR, Auricchio et al. were the first to report FEA results about the deployment of a tubular SG in the thoracic aorta.[25] Derycke et al.[89] have extended the approach to simulate complete deployment of a complex Terumo Aortic® RelayBranch device and its bridging stents in an aneurysmal aortic arch. This recent study showed that the value of simulation of complex SG designs in areas with major collateral arteries appears even greater, considering the severity of complications (such as myocardial infarction, stroke, renal failure, and mesenteric ischemia) associated with side branch coverage or difficult cannulation. This paves the way towards the simulation of total EVAR procedures of the aortic arch[170] and of thoracoabdominal aneurysms.[81] A critical challenge for such procedures is to select branched endograft designs that could fit most aortic arch anatomies. Bosse et al.[74] have explored the use of off-the-shelf endografts, which could be an endovascular therapeutic option to shorten delays related to the design and manufacturing process. Assistance of FEA simulations for total EVAR remains challenging as it requires sophisticated numerical models which still need to be validated on a sufficient number of patients. A further challenge is to achieve real-time computational analyses needed for use of these models in the operating room. For that, the development of reduced-order modeling approaches for virtual EVAR is still a burgeoning field.[24,151]

5 | CONCLUDING REMARKS

EVAR is an evolving field, both in the research arena and clinical practice. Current efforts are directed to SG device optimization, SG device customization, as well as the development of pre- and intra-interventional tools to assist the clinician in the planning and execution of this challenging clinical intervention. The overall goal of these efforts is to reduce EVAR complication rates, and increase the applicability of EVAR to an even wider range of patients requiring aortic aneurysm or dissection treatment.

Predictive capabilities of computational EVAR models, which have been shown for some models on a small patient cohort basis, make the models very promising for future clinical use with a multitude of possible applications. These applications include, among other things, patient-specific prediction of EVAR-related complication likelihoods, as well as individual SG device and EVAR placement and procedure optimization and customization.

Further improvements required for clinical application of computational EVAR models include: achievement of real-time computations by reducing the required computational effort, and complete automation of the process workflow from model generation to the postprocessing of the simulation results. These steps would then allow for the needed large, multicenter studies that evaluate and validate the achievable benefits of such computational augmentation of EVAR procedures. In addition, further model developments such as the prediction of post-EVAR aortic remodeling, could further improve applicability and effectiveness of computational EVAR models. Such improvements could certainly make EVAR modeling an indispensable tool in clinical practice.

Moreover, machine learning and artificial intelligence methods are paving their way to aid in predicting risks and complications based on patient-specific data (history, patient geometry, medications, etc.). Several studies are starting to include these methods (e.g., Dong et al.[175,176]). In the future, use of artificial intelligence will help elucidate relationships between patient data and patient-specific risks. The use of physics-based models, augmented by machine learning and artificial intelligence methods, will allow for personalized medicine approaches enabling physicians to make more informed decisions about patient treatment and interventions.

ACKNOWLEDGMENTS

M.W.G. and A.H. gratefully acknowledge support and funding by the Leibniz Rechenzentrum München (LRZ) of the Bavarian Academy of Sciences under contract number pr48ta. M.W.G. received funding from the German Science Foundation (DFG) under GE 2254/4-1. All authors would like to thank Dr. Sabrina Ben Ahmed for her help in the preparation of Figure 8.

CONFLICT OF INTEREST

S.A. is cofounder of Predisurge SAS, France. S.R. is founder of CirSym, Inc., USA.

ORCID

Stéphane Avril https://orcid.org/0000-0002-8604-7736
Michael W. Gee https://orcid.org/0000-0001-9293-7201
André Hemmler https://orcid.org/0000-0002-1071-8070
Sandra Rugonyi https://orcid.org/0000-0001-9262-7959

REFERENCES

1. Parodi JC, Palmaz JC, Barone HD. Transfemoral intraluminal graft implantation for abdominal aortic aneurysms. *Ann Vasc Surg*. 1991;5:491-499.
2. Patel R, Powell JT, Sweeting MJ, Epstein DM, Barrett JK, Greenhalgh RM. The UKendovascular aneurysm repair (EVAR) randomised controlled trials: long-term follow-up and cost-effectiveness analysis. *Health Technol Assess*. 2018;22:1-132.
3. Patel R, Powell JT, Sweeting MJ, Epstein DM, Barrett JK, Greenhalgh RM. Individual patient data meta-analysis of EVAR trial 1, the dutch randomised endovascular aneurysm management trial, the open versus endovascular repair trial and anévrysme de l'aorte abdominale, chirurgie versus endoprothése trial. In The UK EndoVascular Aneurysm Repair (EVAR) randomised controlled trials: long-term follow-up and cost-effectiveness analysis. *NIHR Journals Library*; 2018.
4. Patel R, Sweeting MJ, Powell JT, Greenhalgh RM, Investigators ET, et al. Endovascular versus open repair of abdominal aortic aneurysm in 15-years' follow-up of the UKendovascular aneurysm repair trial 1 (evar trial 1): a randomised controlled trial. *The Lancet*. 2016;388:2366-2374.
5. Brown L, Powell J, Thompson S, Epstein D, Sculpher M, Greenhalgh R. The UKendovascular aneurysm repair (evar) trials: randomised trials of evar versus standard therapy. In NIHR Health Technology Assessment Programme: Executive Summaries. *NIHR Journals Library*; 2012.
6. Greenhalgh RM. Comparison of endovascular aneurysm repair with open repair in patients with abdominal aortic aneurysm (evar trial 1), 30-day operative mortality results: randomised controlled trial. *Lancet*. 2004;364:843-848.
7. EVAR trial participants. Endovascular aneurysm repair versus open repair in patients with abdominal aortic aneurysm (EVAR trial 1): randomised controlled trial. *The Lancet*. 2005;365:(9478):2179–2186. https://doi.org/10.1016/s0140-6736(05)66627-5
8. Greenhalgh RM, Powell JT. Endovascular repair of abdominal aortic aneurysm. *New Engl J Med*. 2008;358:494-501.
9. Greenhalgh RM, Brown LC, Powell JT. Endovascular versus open repair of abdominal aortic aneurysm. *New Engl J Med*. 2010;362:1863-1871.

10. Mohan IV, Laheij RJF, Harris PL. Risk factors for endoleak and the evidence for stent-graft oversizing in patients undergoing endovascular aneurysm repair. *Eur J Vasc Endovasc Surg*. 2001;21:344-349.
11. Mohan IV, Harris PL, van Marrewijk CJ, Laheij RJ, How TV. Factors and forces influencing stent-graft migration after endovascular aortic aneurysm repair. *J Endovasc Ther*. 2002;9:748-755.
12. Peidro J, Boufi M, Loundou AD, et al. Aortic anatomy and complications of the proximal sealing zone after endovascular treatment of the thoracic aorta. *Ann Vasc Surg*. 2018;48:141-150.
13. Maleux G, Koolen M, Heye S. Complications after endovascular aneurysm repair. *Sem Interv Radiol*. 2009;26:3-9.
14. Schlensak C, Doenst T, Hauer M, et al. Serious complications that require surgical interventions after endoluminal stent-graft placement for the treatment of infrarenal aortic aneurysms. *J Vasc Surg*. 2001;34:198-203.
15. Kouvelos GN, Oikonomou K, Antoniou GA, Verhoeven EL, Katsargyris A. A systematic review of proximal neck dilatation after endovascular repair for abdominal aortic aneurysm. *J Endovasc Ther*. 2017;24:59-67.
16. Chang RW, Goodney P, Tucker L-Y, et al. Ten-year results of endovascular abdominal aortic aneurysm repair from a large multicenter registry. *J Vasc Surg*. 2013;58:324-332.
17. Niestrawska JA, Haspinger DC, Holzapfel GA. The influence of fiber dispersion on the mechanical response of aortic tissues in health and disease: a computational study. *Comput Methods Biomech Biomed Engin*. 2018;21:99-112.
18. van Bakel TMJ, Arthurs CJ, Nauta FJ, et al. Cardiac remodelling following thoracic endovascular aortic repair for descending aortic aneurysms. *Eur J Cardiothorac Surg*. 2019;55:1061-1070.
19. Beebe HG, Cronenwett JL, Katzen BT, et al. Results of an aortic endograft trial: impact of device failure beyond 12 months. *J Vasc Surg*. 2001;33:55-63.
20. Sternbergh WC, Money SR, Greenberg RK, Chuter TA, Investigators Z, et al. Influence of endograft oversizing on device migration, endoleak, aneurysm shrinkage, and aortic neck dilation: results from the zenith multicenter trial. *J Vasc Surg*. 2004;39:20-26.
21. Altnji H-E, Bou-Saïd B, Walter-Le Berre H. Morphological and stent design risk factors to prevent migration phenomena for a thoracic aneurysm: a numerical analysis. *Med Eng Phys*. 2015;37:23-33.
22. Cochennec F, Becquemin JP, Desgranges P, Allaire E, Kobeiter H, Roudot-Thoraval F. Limb graft occlusion following evar: clinical pattern, outcomes and predictive factors of occurrence. *Eur J Vasc Endovasc Surg*. 2007;34:59-65.
23. Kleinstreuer C, Li Z, Basciano C, Seelecke S, Farber M. Computational mechanics of nitinol stent grafts. *J Biomech*. 2008;41:2370-2378.
24. Acosta Santamaría VA, Daniel G, Perrin D, Albertini JN, Rosset E, Avril S. Model reduction methodology for computational simulations of endovascular repair. *Comput Methods Biomech Biomed Engin*. 2018;21:139-148.
25. Auricchio F, Conti M, Marconi S, Reali A, Tolenaar JL, Trimarchi S. Patient-specific aortic endografting simulation: from diagnosis to prediction. *Comput Biol Med*. 2013;43:386-394.
26. Bernardini A, Larrabide I, Morales HG, et al. Influence of different computational approaches for stent deployment on cerebral aneurysm haemodynamics. *Interface Focus*. 2011;1:338-348.
27. Figueroa CA, Zarins CK. Computational analysis of displacement forces acting on endografts used to treat aortic aneurysms. *Biomechanics and Mechanobiology of Aneurysms*. 7. Berlin Heidelberg: Springer-Verlag; 2011:221-246.
28. Figueroa CA, Taylor CA, Yeh V, Chiou AJ, Zarins CK. Effect of curvature on displacement forces acting on aortic endografts: a 3-dimensional computational analysis. *J Endovasc Ther*. 2009;16:284-294.
29. Figueroa CA, Taylor CA, Yeh V, Chiou AJ, Gorrepati ML, Zarins CK. Preliminary 3D computational analysis of the relationship between aortic displacement force and direction of endograft movement. *J Vasc Surg*. 2010;51:1488-1497.
30. Kaladji A, Dumenil A, Castro M, et al. Prediction of deformations during endovascular aortic aneurysm repair using finite element simulation. *Comput Med Imaging Graph*. 2013;37:142-149.
31. Li Z, Kleinstreuer C, Farber M. Computational analysis of biomechanical contributors to possible endovascular graft failure. *Biomech Model Mechanobiol*. 2005;4:221-234.
32. Li Z, Kleinstreuer C. Analysis of biomechanical factors affecting stent-graft migration in an abdominal aortic aneurysm model. *J Biomech*. 2006;39:2264-2273.
33. Li Z, Kleinstreuer C. Blood flow and structure interactions in a stented abdominal aortic aneurysm model. *Med Eng Phys*. 2005;27:369-382.
34. Molony DS, Kavanagh EG, Madhavan P, Walsh MT, McGloughlin TM. A computational study of the magnitude and direction of migration forces in patient-specific abdominal aortic aneurysm stent-grafts. *Eur J Vasc Endovasc Surg*. 2010;40:332-339.
35. Prasad A, Xiao N, Gong X-Y, Zarins CK, Figueroa C. Alberto. A computational framework for investigating the positional stability of aortic endografts. *Biomechanics and Modeling in Mechanobiology*. 2013;12:(5):869-887. https://doi.org/10.1007/s10237-012-0450-3
36. Romarowski R.M., Faggiano E., Conti M., Reali A., Morganti S., Auricchio F. A novel computational framework to predict patient-specific hemodynamics after TEVAR: Integration of structural and fluid-dynamics analysis by image elaboration. *Computers & Fluids*. 2019;179:806-819. https://doi.org/10.1016/j.compfluid.2018.06.002
37. Romarowski RM. Moving computational tools for aortic disease from the bench to the bedside. PhD thesis. University of Pavia; 2018.
38. Roy D, Kauffmann C, Delorme S, Lerouge S, Cloutier G, Soulez G. A literature review of the numerical analysis of abdominal aortic aneurysms treated with endovascular stent grafts. *Comput Math Methods Med*. 2012;1–16:2012.
39. Roy D, Lerouge S, Inaekyan K, Kauffmann C, Mongrain R, Soulez G. Experimental validation of more realistic computer models for stent-graft repair of abdominal aortic aneurysms, including pre-load assessment. *Int J Num Method Biomed Eng*. 2016;32:e02769.
40. Schafer S, Singh V, Noël PB, Walczak AM, Xu J, Hoffmann KR. Real-time endovascular guidewire position simulation using shortest path algorithms. *Int J Comput Assist Radiol Surg*. 2009;4:597-608.

41. van Bogerijen GH, Tolenaar JL, Conti M, et al. Contemporary role of computational analysis in endovascular treatment for thoracic aortic disease. *Aorta*. 2013;1:171.
42. Auricchio F, Conti M, Romarowski RM, De Beaufort HW, Grassi V, Trimarchi S. Computational tools for thoracic endovascular aortic repair planning. *Italian J Vasc Endovas Surg*. 2019;26:51-58.
43. De Bock S. A (bio)mechanical analysis of stent grafts for the treatment of abdominal aortic aneurysms. PhD thesis. Gent University; 2014.
44. Hemmler A, Lutz B, Reeps C, Gee MW. Der digitale Zwilling in der endovaskulären Versorgung. *Gefäßchirurgie*. 2019;24(7):548-556.
45. Hemmler A, Lutz B, Reeps C, Gee MW. Silico study of vessel and stent-graft parameters on the potential success of endovascular aneurysm repair. *Int J Num Method Biomed Eng*. 2019;35(11):e3237. https://doi.org/10.1002/cnm.3237
46. Hemmler A, Lin A, Thierfelder N, Franz T, Gee M, Bezuidenhout D. Customized stent-grafts for endovascular aneurysm repair with challenging necks: a numerical proof of concept. *Int J Num Method Biomed Eng*. 2020;36:4.
47. Hemmler A, Lutz B, Reeps C, Kalender G, Gee MW. A methodology for in silico endovascular repair of abdominal aortic aneurysms. *Biomech Model Mechanobiol*. 2018;17:1139-1164.
48. Hemmler A, Lutz B, Kalender G, Reeps C, Gee MW. Patient-specific in silico endovascular repair of abdominal aortic aneurysms: application and validation. *Biomech Model Mechanobiol*. 2019;18:983-1004.
49. Biehler J, Kehl S, Gee MW, et al. Probabilistic noninvasive prediction of wall properties of abdominal aortic aneurysms using bayesian regression. *Biomech Model Mechanobiol*. 2017;16:45-61.
50. Kuhl E., Maas R., Himpel G., Menzel A.. Computational modeling of arterial wall growth. *Biomechanics and Modeling in Mechanobiology*. 2007;6:(5):321-331. https://doi.org/10.1007/s10237-006-0062-x
51. Lederle FA, Freischlag JA, Kyriakides TC, et al. Outcomes following endovascular vs open repair of abdominal aortic aneurysm: a randomized trial. *JAMA*. 2009;302:1535-1542.
52. Lederle FA, Freischlag JA, Kyriakides TC, et al. Long-term comparison of endovascular and open repair of abdominal aortic aneurysm. *New Engl J Med*. 2012;367:1988-1997.
53. Li S, Qin J, Gao J, Chui Y-P, Heng P-A. A novel fem-based numerical solver for interactive catheter simulation in virtual catheterization. *Journal of Biomedical Imaging*. 2011;3:2011.
54. Menzel A, Kuhl E. Frontiers in growth and remodeling. *Mech Res Commun*. 2012;42:1-14.
55. Molony DS, Callanan A, Kavanagh EG, Walsh MT, McGloughlin TM. Fluid-structure interaction of a patient-specific abdominal aortic aneurysm treated with an endovascular stent-graft. *Biomed Eng Online*. 2009;8:1-12.
56. Morris L, Delassus P, Walsh M, McGloughlin T. A mathematical model to predict the in vivo pulsatile drag forces acting on bifurcated stent grafts used in endovascular treatment of abdominal aortic aneurysms (AAA). *J Biomech*. 2004;37:1087-1095.
57. Niestrawska JA, Viertler C, Regitnig P, Cohnert TU, Sommer G, Holzapfel GA. Microstructure and mechanics of healthy and aneurysmatic abdominal aortas: experimental analysis and modelling. *J Roy Soc Interf*. 2016;13:20160620.
58. Perrin D, Badel P, Orgéas L, et al. Patient-specific numerical simulation of stent-graft deployment: validation on three clinical cases. *J Biomech*. 2015;48:1868-1875.
59. Perrin D, Demanget N, Badel P, et al. Deployment of stent grafts in curved aneurysmal arteries: toward a predictive numerical tool. *Int J Num Method Biomed Eng*. 2015;31:e02698.
60. Perrin D, Badel P, Orgeas L, et al. Patient-specific simulation of endovascular repair surgery with tortuous aneurysms requiring flexible stent-grafts. *J Mech Behav Biomed Mater*. 2016;63:86-99.
61. Polzer S, Gasser TC. Biomechanical rupture risk assessment of abdominal aortic aneurysms based on a novel probabilistic rupture risk index. *J Roy Soc Interf*. 2015;12:20150852.
62. Raghavan ML, Webster MW, Vorp DA. Ex vivo biomechanical behavior of abdominal aortic aneurysm: assessment using a new mathematical model. *Ann Biomed Eng*. 1996;24:573-582.
63. Raghavan M, Vorp DA. Toward a biomechanical tool to evaluate rupture potential of abdominal aortic aneurysm: identification of a finite strain constitutive model and evaluation of its applicability. *J Biomech*. 2000;33:475-482.
64. Polzer S, Kracík J, Novotný T, Kubíček L, Staffa R, Raghavan ML. Methodology for estimation of annual risk of rupture for abdominal aortic aneurysm. *Comput Methods Programs Biomed*. 2021;200:105916.
65. Polzer S, Gasser TC, Vlachovský R, et al. Biomechanical indices are more sensitive than diameter in predicting rupture of asymptomatic abdominal aortic aneurysms. *J Vasc Surg*. 2020;71(2):617-626.
66. De Putter S, Wolters BJBM, Rutten MCM, Breeuwer M, Gerritsen FA, Van de Vosse FN. Patient-specific initial wall stress in abdominal aortic aneurysms with a backward incremental method. *J Biomech*. 2007;40(5):1081-1090.
67. Speelman L, Bosboom EMH, Schurink GWH, et al. Initial stress and nonlinear material behavior in patient-specific AAA wall stress analysis. *J Biomech*. 2009;42(11):1713-1719.
68. Sherifova S, Holzapfel GA. Biomechanics of aortic wall failure with a focus on dissection and aneurysm: a review. *Acta Biomater*. 2019;99:1-17.
69. Gee MW, Reeps C, Eckstein HH, Wall WA. Prestressing in finite deformation abdominal aortic aneurysm simulation. *J Biomech*. 2009;42:1732-1739.
70. Gee MW, Förster C, Wall WA. A computational strategy for prestressing patient-specific biomechanical problems under finite deformation. *Int J Num Method Biomed Eng*. 2010;26:52-72.
71. Bruder L, Pelisek J, Eckstein H-H, Gee MW. Biomechanical rupture risk assessment of abdominal aortic aneurysms using clinical data: a patient-specific, probabilistic framework and comparative case-control study. *PLoS One*. 2020;15(11):e0242097.

72. Maier A, Gee MW, Reeps C, Pongratz J, Eckstein H-H, Wall WA. A comparison of diameter, wall stress, and rupture potential index for abdominal aortic aneurysm rupture risk prediction. *Ann Biomed Eng*. 2010;38:3124-3134.
73. Reeps C, Maier A, Pelisek J, et al. Measuring and modeling patient-specific distributions of material properties in abdominal aortic aneurysm wall. *Biomech Model Mechanobiol*. 2013;12:717-733.
74. Bosse C, Kölbel T, Mougin J, Kratzberg J, Fabre D, Haulon S. Off-the-shelf multibranched endograft for total endovascular repair of the aortic arch. *J Vasc Surg*. 2020;72:805-811.
75. Gasser TC, Ogden RW, Holzapfel GA. Hyperelastic modelling of arterial layers with distributed collagen fibre orientations. *J Roy Soc Interf*. 2006;3:15-35.
76. Holzapfel GA, Ogden RW. Constitutive modelling of arteries. *Proc Roy Soc London A*. 2010;466:1551-1597.
77. Holzapfel GA, Niestrawska JA, Ogden RW, Reinisch AJ, Schriefl AJ. Modelling non-symmetric collagen fibre dispersion in arterial walls. *J Roy Soc Interf*. 2015;12:20150188.
78. Holzapfel GA, Ogden RW, Sherifova S. On fibre dispersion modelling of soft biological tissues: a review. *Proc Royl Soc A*. 2019;475: 20180736.
79. Wolf I, Vetter M, Wegner I, et al. The medical imaging interaction toolkit (MITK)—a toolkit facilitating the creation of interactive software by extending VTK and ITK. Medical imaging 2004: visualization, image-guided procedures, and display. *Proc SPIE*. 2004;5367: 16-27.
80. Yoo TS, Ackerman MJ, Lorensen WE, et al. Engineering and algorithm Design for an Image Processing API: a technical report on ITK—the insight toolkit. In: Westwood J, ed. *Proc. of Medicine Meets Virtual Reality*. IOS Press; 2002:586-592.
81. Verzini F, Loschi D, De Rango P, et al. Current results of total endovascular repair of thoracoabdominal aortic aneurysms. *J Cardiovasc Surg (Torino)*. 2014;55:9-19.
82. Arthurs CJ, Khlebnikov R, Melville A, et al. CRIMSON: an open-source software framework for cardiovascular integrated Modelling and simulation. *PLoS Comput Biol*. 2021;17(5):e1008881.
83. Comaneanu RM, Tarcolea M, Vlasceanu D, Cotrut MC. Virtual 3D reconstruction, diagnosis and surgical planning with mimics software. *Int J Nano Biomater*. 2012;4(1):69-77.
84. https://www.synopsys.com/simpleware/software/scanip.html
85. Auricchio F, Conti M, De Beule M, De Santis G, Verhegghe B. Carotid artery stenting simulation: from patient-specific images to finite element analysis. *Med Eng Phys*. 2011;33:281-289.
86. De Bock S, Iannaccone F, De Santis G, et al. Our capricious vessels: the influence of stent design and vessel geometry on the mechanics of intracranial aneurysm stent deployment. *J Biomech*. 2012;45:1353-1359.
87. De Bock S, Iannaccone F, De Santis G, et al. Virtual evaluation of stent graft deployment: a validated modeling and simulation study. *J Mech Behav Biomed Mater*. 2012;13:129-139.
88. Perrin D. Vers un outil d'aide à la décision pour le traitement des anévrismes par endochirurgie. PhD thesis. Ecole des Mines de Saint Etienne; 2015.
89. Derycke L, Perrin D, Cochennec F, Albertini J-N, Avril S. Predictive numerical simulations of double branch stent-graft deployment in an aortic arch aneurysm. *Ann Biomed Eng*. 2019;47:1051-1062.
90. Derycke L, Sénémaud J, Perrin D, et al. Patient specific computer modelling for automated sizing of fenestrated stent grafts. *Eur J Vasc Endovasc Surg*. 2020;59(2):237-246.
91. Hemmler A. In-silico endovascular repair of abdominal aortic aneurysms. PhD thesis. Technische Universität München; 2020.
92. Demanget N. Analyses des performances mécaniques des endoprothèses aortiques par simulation numérique: application au traitement des anévrismes tortueux. PhD thesis. Ecole des Mines de Saint Etienne; 2012.
93. Demanget N, Avril S, Badel P, et al. Computational comparison of the bending behavior of aortic stent-grafts. *J Mech Behav Biomed Mater*. 2012;5:272-282.
94. Demanget N, Latil P, Orgéas L, et al. Severe bending of two aortic stent-grafts: an experimental and numerical mechanical analysis. *Ann Biomed Eng*. 2012;40:2674-2686.
95. Demanget N, Duprey A, Badel P, et al. Finite element analysis of the mechanical performances of 8 marketed aortic stent-grafts. *J Endovasc Ther*. 2013;20:523-535.
96. Auricchio F, Taylor RL. Shape-memory alloys: modelling and numerical simulations of the finite-strain superelastic behavior. *Computer Methods in Applied Mechanics and Engineering*. 1997;143:(1-2):175-194. https://doi.org/10.1016/s0045-7825(96)01147-4
97. Auricchio F, Taylor RL, Lubliner Jacob. Shape-memory alloys: macromodelling and numerical simulations of the superelastic behavior. *Computer Methods in Applied Mechanics and Engineering*. 1997;146:(3-4):281-312. https://doi.org/10.1016/s0045-7825(96)01232-7
98. Vande Geest JP, Di Martino ES, Bohra A, Makaroun MS, Vorp DA. A biomechanics-based rupture potential index for abdominal aortic aneurysm risk assessment. *Ann N Y Acad Sci*. 2006;1085:11-21.
99. Budd JS, Finch DR, Carter PG. A study of the mortality from ruptured abdominal aortic aneurysms in a district community. *Eur J Vasc Surg*. 1989;3(4):351-354.
100. Schermerhorn ML, Bensley RP, Giles KA, et al. Changes in abdominal aortic aneurysm rupture and short-term mortality, 1995-2008: a retrospective observational study. *Ann Surg*. 2012;256(4):651-658.
101. Sweeting MJ, Ulug P, Powell JT, Desgranges P, Balm R, Trialists RA. Ruptured aneurysm trials: the importance of longer-term outcomes and meta-analysis for 1-year mortality. *Europ J Vasc Endovasc Surg*. 2015;50:297-302.
102. Gwon JG, Kwon TW, Cho YP, Han YJ, Noh MS. Analysis of in hospital mortality and long-term survival excluding in hospital mortality after open surgical repair of ruptured abdominal aortic aneurysm. *Ann Surg Treatment Res*. 2016;91:303-308.

103. Afifi RO, Sandhu HK, Leake SS, et al. Determinants of operative mortality in patients with ruptured acute type a aortic dissection. *Ann Thorac Surg*. 2016;101(1):64-71.
104. Johansson G, Markström U, Swedenborg J. Ruptured thoracic aortic aneurysms: a study of incidence and mortality rates. *J Vasc Surg*. 1995;21(6):985-988.
105. Gindre J, Bel-Brunon A, Kaladji A, et al. Finite element simulation of the insertion of guidewires during an evar procedure: example of a complex patient case, a first step toward patient-specific parameterized models. *Int J Num Method Biomed Eng*. 2015;31:e02716.
106. Gindre J, Bel-Brunon A, Rochette M, et al. Patient-specific finite-element simulation of the insertion of guidewire during an evar procedure: Guidewire position prediction validation on 28 cases. *IEEE Trans Biomed Eng*. 2017;64:1057-1066.
107. Haskett D, Johnson G, Zhou A, Utzinger U, Geest JV. Microstructural and biomechanical alterations of the human aorta as a function of age and location. *Biomech Model Mechanobiol*. 2010;9:725-736.
108. Roccabianca S, Figueroa CA, Tellides G, Humphrey JD. Quantification of regional differences in aortic stiffness in the aging human. *J Mech Behav Biomed Mater*. 2014;29:618-634.
109. Holzapfel Gerhard A., Gasser Thomas C. A viscoelastic model for fiber-reinforced composites at finite strains: Continuum basis, computational aspects and applications. *Computer Methods in Applied Mechanics and Engineering*. 2001;190:(34):4379-4403. https://doi.org/10.1016/s0045-7825(00)00323-6
110. Gasser TC, Görgülü G, Folkesson M, Swedenborg J. Failure properties of intraluminal thrombus in abdominal aortic aneurysm under static and pulsating mechanical loads. *J Vasc Surg*. 2008;48:179-188.
111. TONG J, COHNERT T, REGITNIG P, HOLZAPFEL GA. Effects of age on the elastic properties of the intraluminal thrombus and the thrombus-covered wall in abdominal aortic aneurysms: biaxial extension behaviour and material modelling. *Eur J Vasc Endovasc Surg*. 2011;42:207-219.
112. Maier A Computational modeling of rupture risk in abdominal aortic aneurysms. PhD thesis. TU Munchen; 2012.
113. S. Deputter, F.N. Van De Vosse, M. Breeuwer & F. A. Gerritsen Local influence of calcificationson the wall mechanics of abdominal aortic aneurysm. In: Proc. SPIE, Vol. 6143, SPIE, San Diego, CA, USA; 2006
114. Maier A, Gee MW, Reeps C, Eckstein H-H, Wall WA. Impact of calcifications on patient-specific wall stress analysis of abdominal aortic aneurysms. *Biomech Model Mechanobiol*. 2010;9:511-521.
115. Speelman L, Bohra A, Bosboom EMH, et al. Effects of wall calcifications in patient-specific wall stress analyses of abdominal aortic aneurysms. *J Biomech Eng*. 2007;129:105-109.
116. Huber TS, Wang JG, Derrow AE, et al. Experience in the United States with intact abdominal aortic aneurysm repair. *J Vasc Surg*. 2001;33(2):304-310.
117. Powell JT, Sweeting MJ, Ulug P, et al. Meta-analysis of individual-patient data from EVAR-1, DREAM, OVER and ACE trials comparing outcomes of endovascular or open repair for abdominal aortic aneurysm OVER 5 years. *Br J Surg*. 2017;104(3):166-178.
118. De Bruin JL, Baas AF, Buth J, et al. Long-term outcome of open or endovascular repair of abdominal aortic aneurysm. *New Engl J Med*. 2010;362:1881-1889.
119. van Schaik TG, Yeung KK, Verhagen HJ, et al. Long-term survival and secondary procedures after open or endovascular repair of abdominal aortic aneurysms. *J Vasc Surg*. 2017;66(5):1379-1389.
120. Bastos Gonçalves F, Ultee KH, Hoeks SE, Stolker RJ, Verhagen HJ. Life expectancy and causes of death after repair of intact and ruptured abdominal aortic aneurysms. *J Vasc Surg*. 2016;63(3):610-616.
121. Daye D, Walker TG. Complications of endovascular aneurysm repair of the thoracic and abdominal aorta: evaluation and management. *Cardiovas Diagn Ther*. 2018;8(1):S138-S156.
122. Grootes I, Barrett JK, Ulug P, et al. Predicting risk of rupture and rupture-preventing reinterventions following endovascular abdominal aortic aneurysm repair. *Br J Surg*. 2018;105(10):1294-1304.
123. Li J, Tian X, Wang Z, et al. Influence of endoleak positions on the pressure shielding ability of stent-graft after endovascular aneurysm repair (EVAR) of abdominal aortic aneurysm (AAA). *Biomed Eng*. 2016;15(2):135.
124. Y.H. Lu, K. Mani, B. Panigrahi, W.T. Hsu, C.Y. Chen. Endoleak assessment using computational fluid dynamics and image processing methods in stented abdominal aortic aneurysm models, *Comput Math Method Med*. 2016; 9:9567294.
125. Humphrey J, Holzapfel GA. Mechanics, mechanobiology, and modeling of human abdominal aorta and aneurysms. *J Biomech*. 2012; 45:805-814.
126. Gomes Oliveira NF, Bastos Gonçalves F, Verhagen HJ. Regarding "remodeling of aortic aneurysm and aortic neck on follow-up after endovascular repair with suprarenal fixation". *J Vasc Surg*. 2015;61:840.
127. Ishibashi H, Ishiguchi T, Ohta T, et al. Remodeling of proximal neck angulation after endovascular aneurysm repair. *J Vasc Surg*. 2012; 56:1201-1205.
128. Kwon ST, Rectenwald JE, Baek S. Intrasac pressure changes and vascular remodeling after endovascular repair of abdominal aortic aneurysms: review and biomechanical model simulation. *J Biomech Eng*. 2011;133:011011.
129. Braeu FA, Aydin RC, Cyron CJ. Anisotropic stiffness and tensional homeostasis induce a natural anisotropy of volumetric growth and remodeling in soft biological tissues. *Biomech Model Mechanobiol*. 2019;18:327-345.
130. Schröder J. The mechanical properties of guidewires. Part I: stiffness and torsional strength. *Cardiovasc Intervent Radiol*. 1993;16:43-46.
131. Zarins CK. Stent-graft migration: how do we know when we have it and what is its significance? *J Endovasc Ther*. 2004;11:364-365.
132. Zarins CK, Bloch DA, Crabtree T, Matsumoto AH, White RA, Fogarty TJ. Stent graft migration after endovascular aneurysm repair: importance of proximal fixation. *J Vasc Surg*. 2003;38:1264-1272.

133. Giles KA, Hamdan AD, Pomposelli FB, Wyers MC, Dahlberg SE, Schermerhorn ML. Population-based outcomes following endovascular and open repair of ruptured abdominal aortic aneurysms. *J Endovasc Ther*. 2009;16(5):554-564.
134. Ronellenfitsch U, Meisenbacher K, Ante M, et al. Association between operation volume and postoperative mortality in the elective open repair of infrarenal abdominal aortic aneurysms: systematic review. *Gefässchirurgie*. 2020;25:1-11.
135. Haller SJ, Crawford JD, Courchaine KM, et al. Intraluminal thrombus is associated with early rupture of abdominal aortic aneurysm. *J Vasc Surg*. 2018;67(4):1051-1058.e1.
136. Zelaya JE, Goenezen S, Dargon PT, Azarbal AF, Rugonyi S. Improving the efficiency of abdominal aortic aneurysm wall stress computations. *PLoS One*. 2014;9(7):e101353.
137. Markelj P., Tomaževič D., Likar B., Pernuš F. A review of 3D/2D registration methods for image-guided interventions. *Medical Image Analysis*. 2012;16:(3):642-661. https://doi.org/10.1016/j.media.2010.03.005
138. Kaladji A et al. Safety and accuracy of endovascular aneurysm repair without pre-operative and intra-operative contrast agent. *Eur J Vasc Endovasc Surg*. 2015;49(3):255-261.
139. Stangenberg L et al. A novel tool for three-dimensional roadmapping reduces radiation exposure and contrast agent dose in complex endovascular interventions. *J Vasc Surg*. 2015;62:448-455.
140. Koutouzi G et al. EVAR guided by 3D image fusion and CO_2 DSA: a new imaging combination for patients with renal insufficiency. *J Endovasc Ther*. 2015;22(6):912-917.
141. Maurel B et al. Evaluation of visceral artery displacement by endograft delivery system insertion. *J Endovasc Ther*. 2014;21(2):339-347.
142. Sailer AM et al. CTA with fluoroscopy image fusion guidance in endovascular complex aortic aneurysm repair. *Eur J Vasc Endovasc Surg Off*. 2014;47(4):349-356.
143. Kauffmann C et al. Source of errors and accuracy of a two-dimensional/three-dimensional fusion road map for endovascular aneurysm repair of abdominal aortic aneurysm. *J Vasc Interv Radiol*. 2015;26(4):544-551.
144. Kaladji A et al. Prediction of deformations during endovascular aortic aneurysm repair using finite element simulation. *Spec Issue Mix Real Guid Ther Clin Implement*. 2013;37(2):142-149.
145. Mouktadiri G et al. Aortic endovascular repair modeling using the finite element method. *J Biomed Sci Eng*. 2013;6(9):917-927.
146. Roy D., Holzapfel G. A., Kauffmann C., Soulez G. Finite element analysis of abdominal aortic aneurysms: geometrical and structural reconstruction with application of an anisotropic material model. *IMA Journal of Applied Mathematics*. 2014;79:(5):1011-1026. https://doi.org/10.1093/imamat/hxu037
147. Dumenil Aurelien, Kaladji A., Castro M., Esneault S., Lucas A., Rochette M., Goksu C., Haigron P. Finite-Element-Based Matching of Pre- and Intraoperative Data for Image-Guided Endovascular Aneurysm Repair. *IEEE Transactions on Biomedical Engineering*. 2013;60:(5):1353-1362. https://doi.org/10.1109/tbme.2012.2235440
148. Pionteck A, Pierrat B, Gorges S, Albertini JN, Avril S. Finite-element based image registration for endovascular aortic aneurysm repair. *J Model Eng Sci*. 2020;1(1):22-38.
149. De Bock S, Iannaccone F, De Beule M, et al. Filling the void: a coalescent numerical and experimental technique to determine aortic stent graft mechanics. *J Biomech*. 2013;46:2477-2482.
150. De Bock S, Iannaccone F, De Beule M, Vermassen F, Segers P, Verhegghe B. What if you stretch the IFU? A mechanical insight into stent graft instructions for use in angulated proximal aneurysm necks. *Med Eng Phys*. 2014;36:1567-1576. https://doi.org/10.1016/j.medengphy.2014.08.003
151. Pionteck A, Pierrat B, Gorges S, Albertini JN, Avril S. A fast method of virtual stent graft deployment for computer assisted EVAR. *Computational Biomechanics for Medicine*. Springer; 2019:147-169.
152. Cyron CJ, Aydin RC, Humphrey JD. A homogenized constrained mixture (and mechanical analog) model for growth and remodeling of soft tissue. *Biomech Model Mechanobiol*. 2016;15(6):1389-1403.
153. Cyron CJ, Humphrey JD. Growth and remodeling of load-bearing biological soft tissues. *Meccanica*. 2017;52(3):645-664.
154. Braeu FA, Seitz A, Aydin RC, et al. Homogenized constrained mixture models for anisotropic volumetric growth and remodeling. *Biomech Model Mechanobiol*. 2017;16(3):889-906.
155. Mousavi SJ, Farzaneh S, Avril S. Patient-specific predictions of aneurysm growth and remodeling in the ascending thoracic aorta using the homogenized constrained mixture model. *Biomech Model Mechanobiol*. 2019;18(6):1895-1913.
156. Laubrie JD, Mousavi JS, Avril S. A new finite-element shell model for arterial growth and remodeling after stent implantation. *Int J Num Method Biomed Eng*. 2020;36(1):e3282.
157. Amblard A, Berre HWL, Bou-Saïd B, Brunet M. Analysis of type I endoleaks in a stented abdominal aortic aneurysm. *Med Eng Phys*. 2009;31(1):27-33.
158. Li Z, Kleinstreuer C. Computational analysis of type II endoleaks in a stented abdominal aortic aneurysm model. *J Biomech*. 2006;39(14):2573-2582.
159. Molony DS et al. Geometrical enhancements for abdominal aortic stent-grafts. *J Endovasc Ther*. 2008;15(5):518-529. https://doi.org/10.1583/08-2388.1.eprint
160. Kandail H, Hamady M, Xu XY. Patient-specific analysis of displacement forces acting on fenestrated stent grafts for endovascular aneurysm repair. *J Biomech*. 2014;47(14):3546-3554.
161. Kandail H, Hamady M, Xu XY. Effect of a flared renal stent on the performance of fenestrated stent-grafts at rest and exercise conditions. *J Endovasc Ther*. 2016;23(5):809-820.
162. Kandail H, Hamady M, Xu XY. Comparison of blood flow in branched and fenestrated stent-grafts for endovascular repair of abdominal aortic aneurysms. *J Endovasc Ther*. 2015;22(4):578-590.

163. Mohabbat W, Greenberg RK, Mastracci TM, Cury M, Morales JP, Hernandez AV. Revised duplex criteria and outcomes for renal stents and stent grafts following endovascular repair of juxtarenal and thoracoabdominal aneurysms. *J Vasc Surg*. 2009;49(4):827-837. https://doi.org/10.1016/j.jvs.2008.11.024
164. Ou J, Chan YC, Cheng SW. A systematic review of fenestrated endovascular repair for Juxtarenal and short-neck aortic aneurysm: evidence so far. *Ann Vasc Surg*. 2015;29(8):1680-1688. https://doi.org/10.1016/j.avsg.2015.06.074
165. Tran K, Fajardo A, Ullery BW, Goltz C, Lee JT. Renal function changes after fenestrated endovascular aneurysm repair. *J Vasc Surg*. 2016;64(2):273-280. https://doi.org/10.1016/j.jvs.2016.01.041
166. Martin-Gonzalez T, Pinçon C, Hertault A, et al. Renal outcomes analysis after endovascular and open aortic aneurysm repair. *J Vasc Surg*. 2015;62(3):569-577. https://doi.org/10.1016/j.jvs.2015.03.075
167. LaDisa JF, Olson LE, Molthen RC, et al. Alterations in wall shear stress predict sites of neointimal hyperplasia after stent implantation in rabbit iliac arteries. *Am J Physiol Heart Circ Physiol*. 2005;288(5):H2465-H2475. https://doi.org/10.1152/ajpheart.01107.2004
168. Ullery BW, Suh G-Y, Lee JT, et al. Comparative geometric analysis of renal artery anatomy before and after fenestrated or snorkel/chimney endovascular aneurysm repair. *J Vasc Surg*. 2016;63(4):922-929. https://doi.org/10.1016/j.jvs.2015.10.091
169. Zarins CK, Taylor CA. Endovascular device Design in the Future: transformation from trial and error to computational design. *J Endovasc Ther*. 2009;16(1):12-21. https://doi.org/10.1583/08-2640.1.eprint
170. Rudarakanchana N, Jenkins M. Hybrid and total endovascular repair of the aortic arch. *Br J Surg*. 2018;105:315-327. https://doi.org/10.1016/j.compbiomed.2013.01.006
171. Yuan X, Kan X, Xu XY, Nienaber CA. Finite element modeling to predict procedural success of thoracic endovascular aortic repair in type A aortic dissection. *JTCVS Tech*. 2020;4:40-47. https://doi.org/10.1016/j.xjtc.2020.10.006
172. Tran K, Yang W, Marsden A, Lee JT. Patient-specific computational flow modelling for assessing hemodynamic changes following fenestrated endovascular aneurysm repair. *JVS Vasc Sci*. 2021;2:53-69. https://doi.org/10.1016/j.jvssci.2020.11.032
173. Liu MY, Jiao Y, Liu J, Zhang S, Li W. Hemodynamic parameters predict in-stent thrombosis after multibranched endovascular repair of complex abdominal aortic aneurysms: a retrospective study of branched stent-graft thrombosis. *Front Cardiovasc Med*. 2021;8:654412. https://doi.org/10.3389/fcvm.2021.654412
174. Tan WT, Liew YM, Mohamed Mokhtarudin MJ, et al. Effect of vessel tortuosity on stress concentration at the distal stent-vessel Interface: possible link with new entry formation through biomechanical simulation. *J Biomech Eng*. 2021;143(8):081005. https://doi.org/10.1115/1.4050642
175. Dong Y, Que L, Jia Q, et al. Predicting reintervention after thoracic endovascular aortic repair of Stanford type B aortic dissection using machine learning. *Eur Radiol*. 2021;143(8):1-9. https://doi.org/10.1007/s00330-021-07849-2
176. Zhou M, Shi Z, Li X, et al. Prediction of distal aortic enlargement after proximal repair of aortic dissection using machine learning. *Ann Vasc Surg*. 2021. https://doi.org/10.1016/j.avsg.2021.02.039
177. Vignon-Clementel IE, Figueroa CA, Jansen KE, Taylor CA. Outflow boundary conditions for 3D simulations of non-periodic blood flow and pressure fields in deformable arteries. *Comput Methods Biomech Biomed Engin*. 2010;13(5):625-640. https://doi.org/10.1080/10255840903413565

How to cite this article: Avril S, Gee MW, Hemmler A, Rugonyi S. Patient-specific computational modeling of endovascular aneurysm repair: State of the art and future directions. *Int J Numer Meth Biomed Engng*. 2021;37(12):e3529. doi:10.1002/cnm.3529